Magnetic Properties of Iron(III) Complexes with Photoisomerizable Ligands

Shigeyuki Hirose, Shinya Hayami, and Yonezo Maeda*

Department of Chemistry and Physics of Condensed Matter, Graduate School of Sciences, Kyushu University, Hakozaki, Higashi-ku, Fukuoka 812-8581

(Received April 7, 2000)

New spin-crossover Iron(III) complexes [Fe(salten)(*trans*-stpy)]BPh_4·$(CH_3)_2CO$·$0.5H_2O$ **1** and [Fe(salten)(*cis*-stpy)]-BPh_4 **2** with *cis–trans* photoisomerizable ligands have been synthesized and characterized, where *trans*-stpy is *trans*-4-styrylpyridine and *cis*-stpy *cis*-4-styrylpyridine, and salten denotes bis(3-salicylideneaminopropyl)amine, which is a quinquedentate Schiff base derived from the condensation of salicylaldehyde and di(3-aminopropyl)amine. The data of the variable-temperature magnetic susceptibility measurements for the complexes show that **1** and **2** exhibit spin-crossover phenomena in a solid. The spin-state transition temperature of **1** is lower than that of **2**. The temperature dependencies of the Mössbauer spectra for the complexes also provide evidence that spin-state transitions between the high- and low-spin states take place, and that the rates of the spin interexchange at 298 K are faster than the inverse of the lifetime (1×10^{-7} s) of the Mössbauer nucleus. A temperature dependence of the UV-visible spectra suggesting spin-equilibrium in acetonitrile solution was obtained. The X-ray diffraction structures of single crystals of **1** and **2** were determined. Crystal data for **1**: $C_{60}H_{61}N_4O_{3.5}FeB$, space group $P\bar{1}$ (#2), $Z = 2$, $a = 14.83(1)$, $b = 17.98(1)$, $c = 11.31(2)$ Å, $\alpha = 103.71(8)$, $\beta = 110.60(8)$, $\gamma = 94.31(7)°$, $V = 2702(5)$ Å^3, $R = 14.0\%$, $R_w = 17.2\%$. Crystal data for **2**: $C_{57}H_{54}N_4O_2FeB$, space group $P2_1/n$ (#14), $Z = 4$, $a = 14.823(9)$, $b = 17.417(7)$, $c = 18.37(1)$ Å, $\beta = 95.331(8)°$, $V = 4722(3)$ Å^3. The coordination cores of both complexes have *trans* coordination in oxygen atoms. Although light irradiation to **1** in acetonitrile brings about isomerization from *trans*- to *cis*- of styrylpyridine, the change in the spin-state of the complexes is not clear.

Tanabe and Sugano calculated the energy levels of d^n electronic configurations in an octahedral ligand field.[1] According to the diagram for the d^5 configuration, the ground state changes from ^6A to ^2T at a crossover point when the ligand field strength (Dq/B) is increased, and therefore there are three types of iron(III) complexes in the octahedral field depending on the ligand field strength, high-spin (HS) state ^6A, low-spin (LS) state ^2T and spin-crossover ($^2T \rightleftarrows {}^6A$). A number of spin-crossover complexes have been studied, and it has become clear that the magnetic behaviors of the spin-crossover complexes in a solid are influenced by the molecular packing, hydrogen bonding, polarization of ions, charge transfer in cations and electrostatic energy configurations.[2—4] A spin-state transition is driven by the irradiation of light as well as by the temperature or pressure. In 1984, Gütlich et al.[5] discovered the phenomenon of a quantitative light-induced $^1A_1$ (LS) $\rightarrow {}^5T_2$ (HS) transformation at a temperature much lower than that of the thermal transition in $[Fe(ptz)_6](BF_4)_6$ (ptz: 1-propyltetrazole) and $[Fe(2\text{-pic})_3]Cl_2$·EtOH (2-pic: 2-(aminoethyl)pyridine) in solid state. This phenomenon means that the metastable HS state produced by irradiating the sample into the spin-allowed d–d or MLCT absorption bands of the stable LS species can remain trapped with a practically infinite lifetime.[5] This effect is termed "light-induced excited spin-state trapping", abbreviated as LIESST. A study of this effect has been the subject of an extensive investigation in the field of coordination chemistry. The incorporation of a photoresponsive component into a supramolecular structure can lead to a artificial photoresponsive species.[6]

As a new phenomenon, Zarembowitch et al.[7] have reported that they were working with the object to induce a reversible change of the spin state of the transition metal ions in a complex, according to a new strategy which consists of varying the ligand-field strength under the effect of electromagnetic radiation. This phenomenon should lead to the occurrence of a photochemically-triggered electronic spin-state crossover at relatively high temperatures. This effect is termed "ligand-driven light-induced spin change" (LD-LISC). The process is based on the utilization of ligands capable of taking part in photoreactions, such as *cis–trans* photoisomerizable ligands. The first observation of a LD-LISC effect was reported for $Fe(stpy)_4[(B(CN)(Ph)_3]$ by Zarembowitch et al.,[7c] where stpy is a *cis–trans* photoisomerizable ligand, 4-styrylpyridine. A complex with *trans*-stpy undergoes a thermally-induced spin-crossover centered at around 190 K, and that with *cis*-stpy remains in the HS state at any temperature. The photoisomerization of *trans*-stpy in a complex embedded within a cellulose acetate matrix at 140 K is effectively shown on the basis of UV-vis absorption measurements to trigger a spin-state change of the iron(II) ions.

Matsumoto et al.[8] have reported a series of spin-crossover iron(III) complexes with the general formula $[Fe(salten)(L)]^{n+}$ ($n = 0$, 1). The spin-state of iron(III) ions of the complexes depends on the sixth ligand, L. It is possible for

these complexes to induce a spin change of the iron(III) ions by a slight variation of the ligand-field strength of the sixth ligand. In this paper, the synthesis, magnetic properties and photochemistry of [Fe(salten)(L)]BPh_4 with photoisomerizable ligand 4-styrylpyridine are described.

Results and Discussion

Single Crystal X-Ray Structures. The single-crystal structures of **1** and **2** were determined by single-crystal X-ray diffraction at 296 K. The results for both complexes were not good because the *R* values were high. However, the forms of the molecules could be clearly visualized, the ORTEP drawings of the cations with the numbering of the atoms for **1** and **2** are shown in Figs. 1 and 2, respectively. The crystallographic data for **1** are given in Table 1, and the final positional atomic parameters are given in the Table II in the supplement. The crystallographic data and the positional parameters for **2** are given in the Table I and III in the supplement, respectively. A listing of selected bond distances and angles for **1** and **2** is given in Table IV in the supplement.

Complex **1** crystallizes in the $P\bar{1}$ (#2) triclinic space group ($Z = 2$). The photoisomerizable ligand styrylpyridine exists in *trans* geometry, as shown in Fig. 1. Although solvents, acetone and water are contained in the crystal, no hydrogen bonding exists in the complexes. On the other hand, **2** crystallizes in the $P2_1/n$ (#14) monoclinic space group ($Z = 4$). The photoisomerizable ligand styrylpyridine exists in *cis* geometry. Each iron atom has a pseudo-octahedral coordination with a *trans* geometry in oxygen atoms and the two axial positions are occupied by the secondary amine nitrogen atom of di(3-aminopropyl)amine and the nitrogen

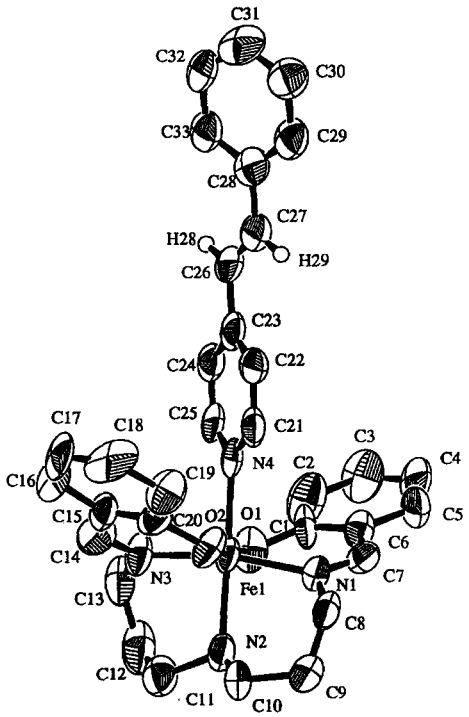

Fig. 1. Ortep drawing of the cation with the numbering of the atoms for **1**.

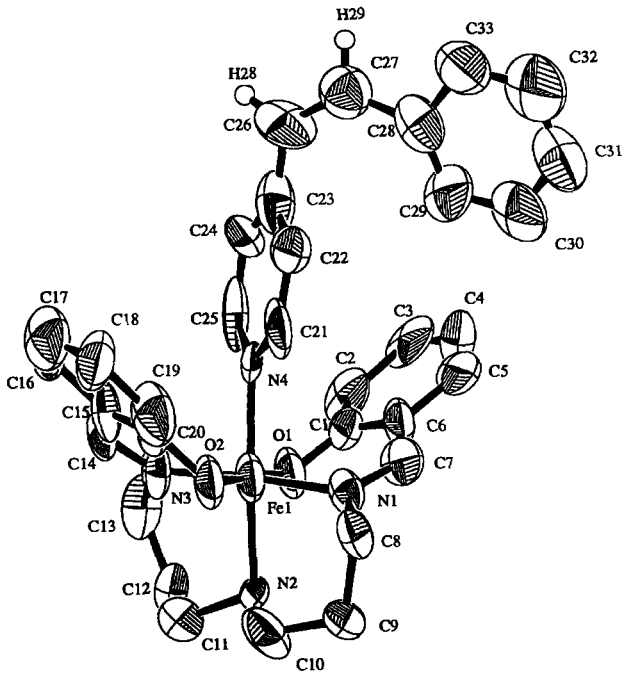

Fig. 2. Ortep drawing of the cation with the numbering of the atoms for **2**.

Table 1. Crystallographic Data for **1**

Empirical formula	$C_{60}H_{61}N_4O_{3.5}BFe$
Formula weight	960.827
Crystal color, Habit	Violet, Prismatic
Crystal dimensions	$0.20 \times 0.10 \times 0.30$ mm
Crystal system	Triclinic
Lattice type	Primitive
Lattice parameters	$a = 14.83(1)$ Å
	$b = 17.98(1)$ Å
	$c = 11.31(2)$ Å
	$\alpha = 103.71(8)°$
	$\beta = 110.60(8)°$
	$\gamma = 94.31(7)°$
	$V = 2702(5)$ Å^3
Space group	$P\bar{1}$ (#2)
Z value	2
D_{calc}/g cm^{-3}	1.181
μ (Mo $K\alpha$)	3.27 cm^{-1}
Diffractometer	Rigaku AFC7R
Radiation	Mo $K\alpha$ ($\lambda = 0.71069$ Å)
	Graphite monochromated
Scan type	ω–2θ
No. of reflection measured	Total: 10690
	Unique: 10287 ($R_{int} = 0.074$)
Structure solution	Direct methods (SAPI91)
p-factor	0.01
No. observations ($I > 3.00\sigma(I)$)	3889
No. variables	657
Residuals: R;[a] R_w[b]	0.140; 0.172
Goodness of fit indicator	3.20

a) $R = \sum||F_o| - |F_c||/\sum|F_o|$.

b) $R_w = [\sum w(|F_o| - |F_c|)^2/\sum wF_o^2]^{\frac{1}{2}}$.

atom of 4-styrylpyridine. The FeN_4O_2 core is less distorted in **2** than in **1**. It is known that the iron-coordinating atom distances for iron(III) complexes with porphyrin derivatives, dialkyldithiocarbamates, or sexidentate Schiff-base ligands are affected by the spin state of iron(III).[9] The average iron-coordinating atom distance in the high-spin complexes, ca. 2.06 Å, is longer by ca. 0.12 Å than that in the LS complexes, 1.94 Å. The magnetic moments for **1** and **2** are 5.13 and 3.17 B.M. at the temperature which the X-ray diffraction study was performed, respectively. The representative bond distances for **1** and **2** are listed in Table 2 and the average iron- coordinating atom distance in **1** is 2.04 Å, close to those for the high-spin complexes. The average iron-coordinating atom distance in **2** is 1.98 Å, being intermediate between the high- and low- spin complexes.

Magnetic Susceptibilities. The temperature dependencies of the effective magnetic moments of **1** and **2** are shown in Fig. 3. The values of the magnetic moments of the complexes are 5.13 B.M. at 290 K and 2.00 B.M. at 80 K for **1**. The effective magnetic moments of **1** gradually increase from the typical values for the low-spin state at 80 K to values close to the high-spin states at 350 K, exhibiting a thermally induced $S = \frac{1}{2} \leftrightarrow S = \frac{5}{2}$ spin-crossover centered at ca. 260 K, evaluated by assuming that μ_h is 5.92 B.M. and μ_l 1.73 B.M. The effective magnetic moments of **2** gradually increase from 2.35 B.M. at 80 K to 4.26 B.M. at 350 K with an increase in the temperature. The curve of the magnetic moments of **2** also exhibits a spin-crossover behavior, although the transition is very gradual compared with that of **1**. The spin-state transition to the high-spin state is not completed, even at 350 K. The magnetic moments in acetonitrile solution are 3.47 B.M. for **1** and 4.22 B.M. for **2** at 293 K.

Table 2. Representative Bond Distances (Å) for **1** and **2**

1		**2**	
Bond distances (Å)			
Fe(1)–O(1)	1.91(2)	Fe(1)–O(1)	1.92(1)
Fe(1)–O(2)	1.92(2)	Fe(1)–O(2)	1.91(1)
Fe(1)–N(1)	2.06(1)	Fe(1)–N(1)	1.96(1)
Fe(1)–N(2)	2.13(2)	Fe(1)–N(2)	2.06(1)
Fe(1)–N(3)	2.04(1)	Fe(1)–N(3)	2.00(1)
Fe(1)–N(4)	2.15(1)	Fe(1)–N(4)	2.05(1)

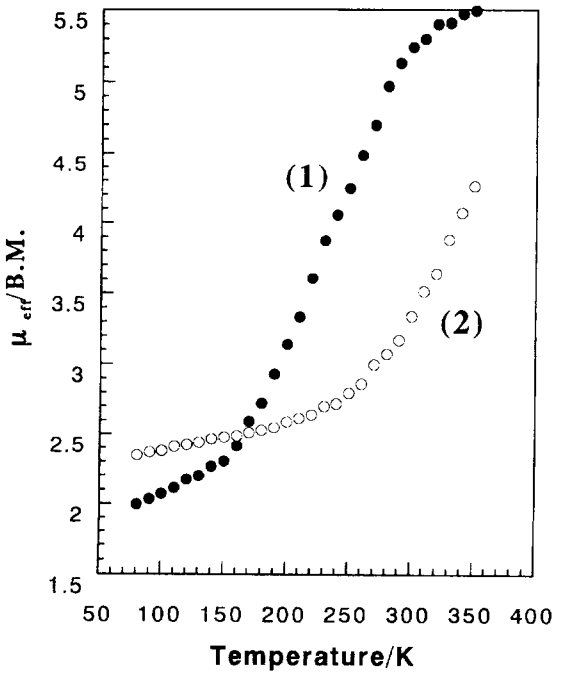

Fig. 3. Temperature dependencies of the effective magnetic moments of **1** and **2**.

Mössbauer Spectra. The Mössbauer spectra of **1** and **2** were measured at various temperatures and are shown in Figs. 4 and 5, respectively. The Mössbauer spectra of **1** and **2** were all analyzed as a pair of doublet; the parameters derived are collected in Table 3. The quadrupole splitting (ΔE_q) values of **1** decrease with increasing the temperature, and the isomer shift (δ) at 78 K is close to the typical values for the low-spin state. Although the isomer shift at 293 K 0.33 mm s^{-1} is not too large compared to 0.29 mm s^{-1}, it is larger than 0.29 mm s^{-1}. The values of the isomer shifts at high temperature should be lower than those at low temperature because of the second-order Doppler shift, if the electronic state of irons at high temperature is in the same spin-state as that at low temperature. Therefore, the isomer shift of 0.33 mm s^{-1} is assigned to that of the high-spin state. In

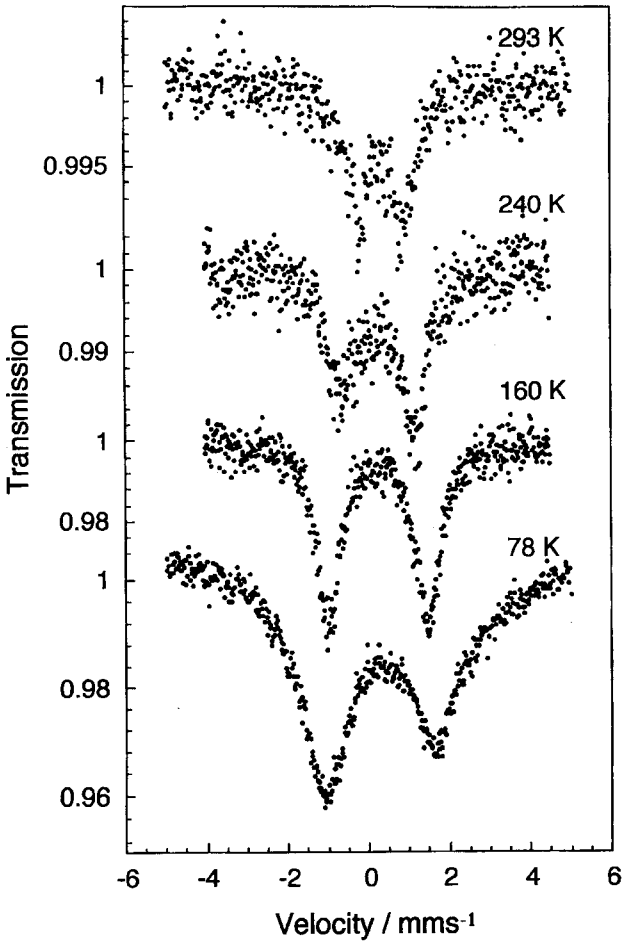

Fig. 4. Temperature dependence of the Mössbauer spectra of **1**.

Table 3. Mössbauer Parameters for the Complexes[a)]

Complexes	T/K	δ/mm s^{-1}	ΔE_q/mm s^{-1}	Γ_+/mm s^{-1}	Γ_-/mm s^{-1}	$\sum\chi^2/\times10^{-4}$
1	293	0.33	1.09	0.72	0.70	7.49
	240	0.26	1.73	0.77	1.07	32.35
	160	0.24	2.46	0.75	0.68	47.91
	78	0.29	2.74	1.99	1.50	17.89
2	293	0.17	1.36	0.37	0.35	13.98
	78	0.34	2.26	2.09	1.40	33.58

a) δ: Isomer shift relative to iron, ΔE_q: Quadrupole splitting, Γ_+ and Γ_-: Full widths at half-maximum for high energy line and low energy line, respectively. $\sum\chi^2$: Residual sum.

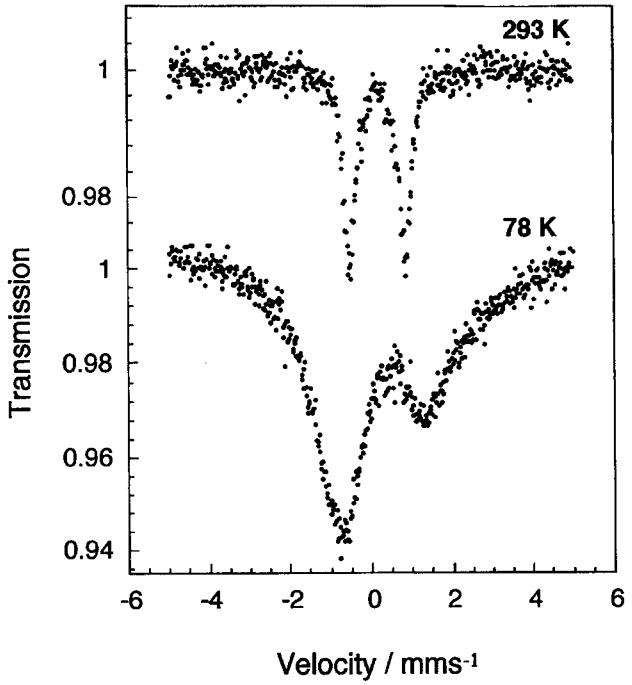

Fig. 5. Temperature dependence of the Mössbauer spectra of **2**.

the temperature range from 200 to 270 K where the isomer shifts markedly increase, the ΔE_q values decrease according to the increase in the population of the high-spin state. The Mössbauer spectrum of **2** at 293 K is characterized by a well-resolved doublet with δ = 0.17 mm s^{-1} and ΔE_q = 1.36 mm s^{-1}. The value of 3.17 B.M. for **2** at 290 K suggests that the complex includes ca. a 20% high-spin fraction of the iron(III) complex. The spectrum at 78 K shows a very broad antisymmetric doublet with δ = 0.34 mm s^{-1}, ΔE_q = 2.26 mm s^{-1}, Γ_+ = 2.09 mm s^{-1} and Γ_- = 1.40 mm s^{-1}, being assigned to the low-spin state. The value of the isomer shift at 293 K 0.17 mm s^{-1} is smaller than 0.34 mm s^{-1} at 78 K, being due to the small population of the high-spin state at 293 K. Therefore, the nucleus strongly feels the second-order Doppler shift more than the difference in the electron density at the nucleus between the high-spin and low-spin states. The antisymmetric broad doublet at 78 K suggests that spin–spin relaxation effects on $^2T_2$ may be induced because of the long Fe–Fe distance due to the presence of bulky anions, BPh_4^-. We expect that the lattice relaxation of the ion is slow compared with the spin–spin relaxation, since each iron is separated with long distance due to bulky anions. The spin–spin relaxation causes the ion to make transitions between the different sublevels; these transitions produce an randomly varying time-dependent magnetic field at the nucleus, and make a broad antisymmetric doublet.[10] Only one doublet is observed in the spectra of **2** at 293 K in spite of the intermediate values between the high- and low-spin states in the magnetic moments. This observation suggests that the rate of the spin-state interexchange between the high- and low-spin states is faster than the inverse of the lifetime of the excited state of a Mössbauer nuclide ^{57}Fe (1×10^{-7} s); therefore, the spectra of the averaged electronic state are observed. A similar spectra with a rapid interexchange between the high- and low-spin states have been observed for [Fe(salten)(2Me-im)]BPh_4.[8a]

Absorption Spectra in Acetonitrile Solution. The temperature dependencies of the absorption spectra in acetonitrile solution were measured, and are shown in Fig. 6 for **1** and in Fig. 7 for **2**. The salten complexes containing pyridine derivatives as an axial ligand are known to show a thermochromic behavior in various organic solvents, changing in color from dark violet to blue green upon a decrease in temperature.[8] The absorption spectra of [Fe(salten)(py)]-BPh_4 in CH_2Cl_2 show a spin-crossover behavior, depending

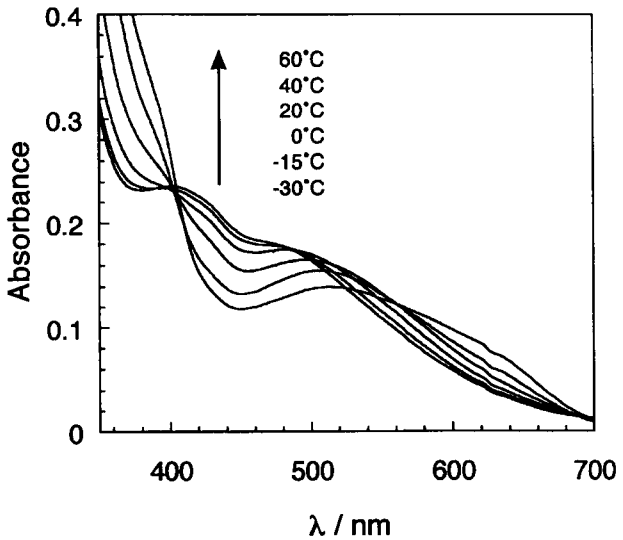

Fig. 6. Temperature dependence of the absorption spectra of **1** in acetonitrile (5×10^{-5} M).

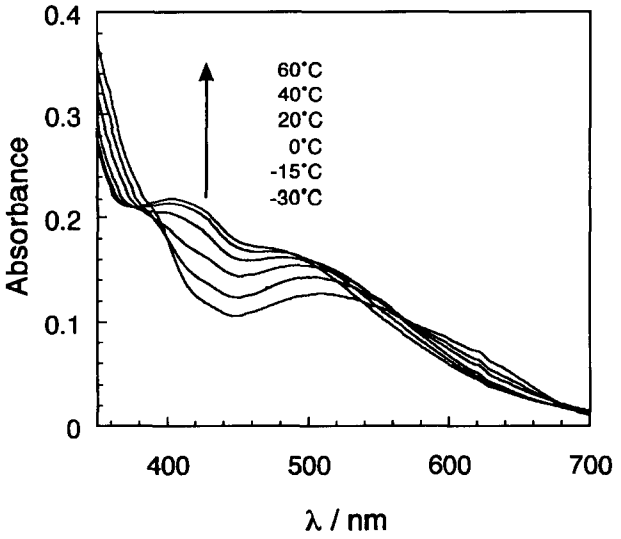

Fig. 7. Temperature dependence of the absorption spectra of **2** in acetonitrile solution (5×10^{-5} M).

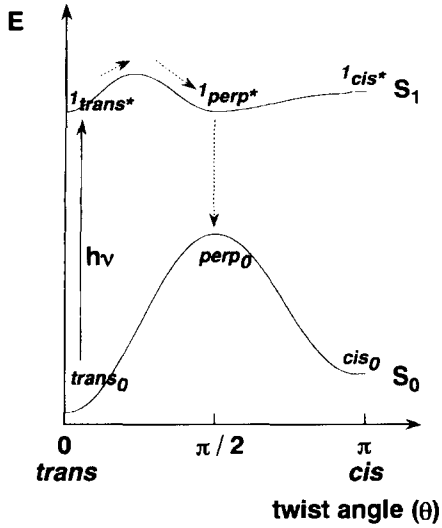

Scheme 1. Potential energy diagram for the lowest singlet state of stilbene as a function of the double bond rotation.

on the temperature, and the absorption at 430 nm decreases in intensity, while that at 510 nm shifts to a longer wavelength with a decrease in intensity upon decreasing temperature. Therefore, the absorption bands at longer wavelength are assigned to the charge transfer (CT) band of the low-spin species, and those at shorter wavelength are assigned to the CT band of the high-spin species. Similar CT bands (430 nm for high-spin species and 490 nm for low-spin species, the latter peak shifts to as observed here) are observed for [(salten)Fe(bpy)Fe(salten)](BPh$_4$)$_2$ (bpy: 4,4′-bipyridine).[11] The spectrum at −30 °C for **1** (Fig. 6) exhibits an absorption at ca. 520 nm with an extinction coefficient of ε = 2800 mol^{-1} dm^3 cm^{-1}. Upon increasing the temperature, the absorption peak at ca. 520 nm shifts to a shorter wavelength along with an increase in the intensity, and a new peak appears at ca. 410 nm. The changes in the spectra with temperature show spin-equilibrium between the high-spin and low-spin states. It can be considered that the high-spin species shows absorption at ca. 410 nm, and the low-spin species at ca. 520 nm. The spectral change is associated with a pseudo-isosbestic point at ca. 400 nm and the peak at 520 nm is gradually displaced to a shorter wavelength with an increase in the temperature. Complex **2** shows a pseudo isosbestic point at 380 nm; the shift of the isosbestic point is remarkable compared with that of **1**.

Photoisomerization. Since a light-induced excited state of 4-styrylpyridine[12] is unstable, it can easily react at room temperature, even if in the case where the ground state can not react thermochemically. The potential curves of the ground and excited states of stilbene are well known, and are shown in Scheme 1 as a function of the twist angles around the double bond. The peak of the potential curve of the ground state in a change from *trans* to the *cis* form is considerably high (ca. 70 kcal mol^{-1}). The *cis* form can be easily produced through the ^{1}*trans** → ^{1}*perp** → *perp*$_0$ pathway by the irradiation of light at λ_{exc} = 313 nm at room temperature, although it is impossible to produce the *cis* form from the *trans* one with a heat reaction (Scheme 1). The *perp* state represents that one phenyl group is perpendicular to the other. The excited singlet state is relaxed to *perp*$_0$, and, finally, *trans*$_0$ and *cis*$_0$ are produced with the ratio of α to $(1-\alpha)$ by deactivation, where α and $1-\alpha$ are the decay fraction from the twisted singlet configuration to the *trans*$_0$ and *cis*$_0$ sides, respectively. The ratio depends on various factors: the ratio of the formation rate of the *cis* to *trans* form, their energies and so on.

The *cis–trans* photoisomerization of uncoordinated styrylpyridine in solution has been widely investigated.[13–16] The $\Phi_{t\to c}$ quantum yield with λ_{exc} = 313 nm is 0.46 in acetonitrile at room temperature.[12] The *cis* isomers lead to a dihydropolycyclic compound as cyclization besides *cis* → *trans* isomerization upon irradiation with λ_{exc} = 254 nm.[13,15] However, this reaction is reversible in the absence of oxidants. Because irradiation with λ_{exc} = 313 nm is slightly absorbed by the *cis* isomers, there is little cyclization and back isomerization.

Irradiation of the Ligands. The changes in the absorption spectra of *trans*-4-styrylpyridine and *cis*-4-styrylpyridine in acetonitrile upon irradiation with λ_{exc} = 313 nm are shown in Fig. 8. *Trans*-stpy shows a characteristic absorption at 299 nm with ε = 25300 mol^{-1} dm^3 cm^{-1}, of which the intensity decreases with the irradiation time; the position of the maximum absorption shifts to a shorter wavelength with a decrease in the intensity, at 285 nm with ε = 10200 mol^{-1} dm^3 cm^{-1}, and an increase in the absorption around 250 nm is observed. A photostationary state is obtained after 90 s-irradiation. On the other hand, the maximum peak with ε = 9930 mol^{-1} dm^3 cm^{-1} for *cis*-stpy is observed at 278 nm and the spectrum of irradiated *trans*-stpy is very similar to that of *cis*-stpy. These data indicate that the change in the spectrum of *trans*-stpy with light irradiation is attributed to *trans* → *cis* isomerization, and that ca. 90% of the *trans*-stpy (5×10^{-5} M, 1 M = 1 mol dm^{-3}) isomerizes to *cis*-stpy in 90 s in acetonitrile. The irradiated ligand was kept at room

temperature for some days. The reverse reaction from *cis* to *trans* was not observed, even if the irradiated samples were annealed at 40 °C or were irradiated with light of λ_{exc} = 460 nm.

Irradiation of the Complexes in Solution. Because complexes **1** and **2** are geometrical isomers (*trans–cis*) of each other, the value of the magnetic moment of **1** in acetonitrile (3.47 B.M. (ca. 26% HS)) is different from that of **2** (4.22 B.M. (ca. 45% HS)) at 293 K. Therefore, the spin-state transition of the complexes may be observed according to whether stpy is in the *trans* or *cis* configuration. The change in the absorption spectra of **1** in acetonitrile accompanying 313 nm irradiation is shown in Fig. 9. The peak with ε = 35500 mol^{-1} dm^3 cm^{-1} in the initial spectrum is observed at 304 nm, which decreases in intensity with the irradiation of light, being attributed to *trans* → *cis* photoisomerization. This observation is similar to the case of *trans*-stpy (Fig. 8). The *trans* → *cis* photoisomerization is almost completed in 4 min of irradiation. In the region 400—600 nm, attributed to the CT band, little changes are observed in the spectra. The temperature dependence of the absorption spectrum of the irradiated **1** in acetonitrile was measured, and is shown in Fig. 10. The spectra show an isosbestic point at ca. 400 nm, of which the position is close to that of the unirradiated **1**; an isosbestic point of the unirradiated **2** is shown at ca. 380 nm (Fig. 7). This observation confirms that the irradiated **1** shows the same spin-crossover behavior as the unirradiated one; nevertheless, the axial ligand *trans*-stpy changes to *cis*-stpy. Why does the irradiated **1** not show a similar spin-crossover behavior to **2**? The phenyl group of stpy in **2** falls to the O2–N1 direction, as shown in Fig. 2. When *trans*-stpy changes to *cis*-stpy in acetonitrile, the phenyl group of stpy falls in the O2–N1 direction or the O1–N3 one. If the phenyl group falls to the O1–N3 direction upon irradiation, the spin-state of the complexes would be different from that of **2**. In any case, there is a possibility that the coordination geometry of the iron site of the irradiated **1** is not the same as that of **2**, and the irradiated **1** is not decomposed by irradiation, because the solution spectra of the irradiated 1 show a spin-crossover behavior.

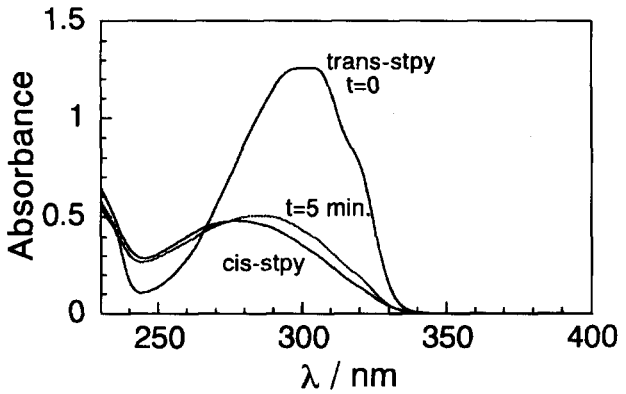

Fig. 8. The change in the absorption spectra of *trans*-stpy with 313 nm irradiation and the absorption spectrum of *cis*-stpy in acetonitrile (5×10^{-5} M).

Irradiation of the Complexes in Solid State. Irradiation was tried for **1** and **2** in a KBr disk. Complex **1** (0.4 mg) was mixed with KBr (200 mg) and the mixed samples were used as a disk. The change in the absorption spectrum of **1** in the KBr disk accompanying irradiation with λ_{exc} = 313 nm is shown in Fig. I along with the spectrum of the unirradiated **2** in the supplemental. Irradiation with λ_{exc} = 313 nm was continued until a photostationary state was reached. A decrease in the intensity is observed at ca. 300 nm for **1**, being due to *trans* → *cis* photoisomerization with irradiation, but the decrease of the CT band at ca. 520 nm is not clear. The degree of the change is not pronounced, because the change in *trans* → *cis* photoisomerization is smaller than that in acetonitrile and/or because the spin-state of the complexes is not changed by irradiation.

Conclusion

The new Fe(III) complexes exhibiting a thermally-induced spin-crossover behavior both in solid and in acetonitrile have been synthesized. The spin-state transition of the complex **1**

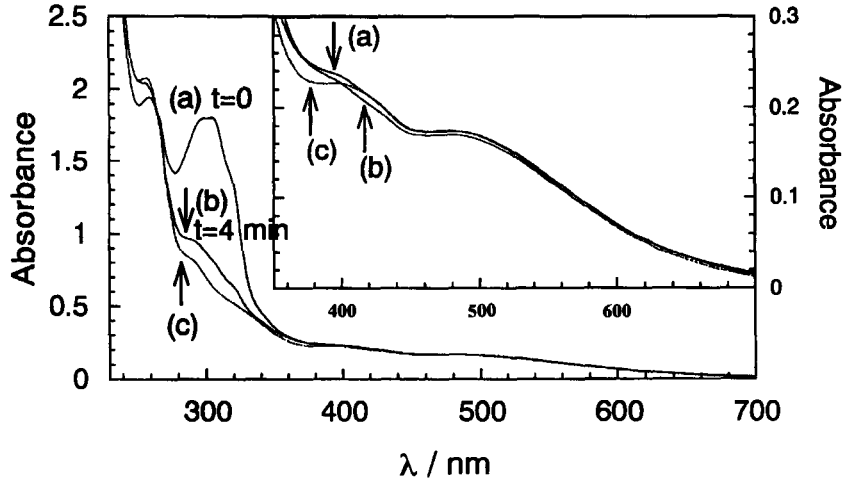

Fig. 9. Absorption spectra in acetonitrile (5×10^{-5} M) at 293 K of (a): the complex **1**, (b): the 313 nm irradiated **1** for 4 min, and (c): the unirradiated **2**.

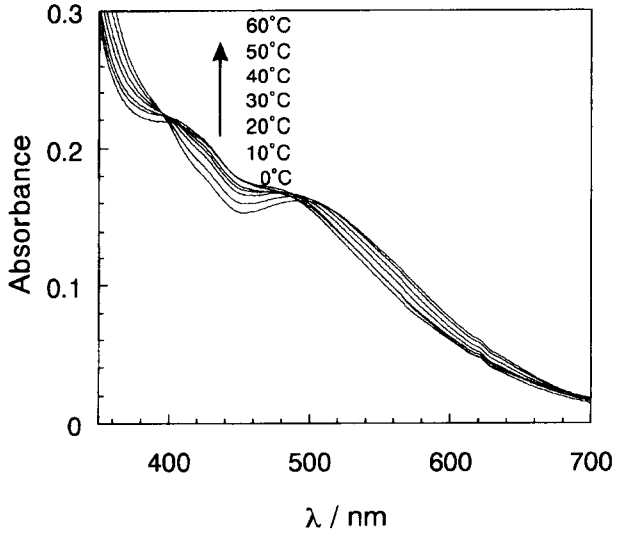

Fig. 10. Temperature dependence of the absorption spectra of the 313 nm irradiated **1** in acetonitrile (5×10^{-5} M).

has been almost completed in the temperature range studied (80—350 K); on the other hand, complex **2** has exhibited a gradual spin-equilibrium, which seems to be completed at a wider temperature range than 80—350 K. These magnetic behaviors have been confirmed by the temperature dependence of the Mössbauer spectra, which show a rapid spin-state interexchange ($> 1\times10^{-7}$ s). These complexes contain the *trans–cis* photoisomers and exhibit different magnetic moments from each other. These spin states have been supported by single-crystal X-ray structure analyses. The average bond lengths of Fe-coordinating atoms for **1** and **2** are 2.04 and 1.98 Å, respectively, and the FeN_4O_2 core is less distorted in **2** than in **1**. Light irradiation to **1** brings about isomerization from *trans-* to *cis-* of styrylpyridine, but the change in the spin-state of the complexes is not clear.

Experimental

Preparation of the Ligands. All of the chemicals and solvents used for the syntheses were of reagent grade.

***trans*-4-Styrylpyridine:**[17] A solution of 4-methylpyridine (0.3 mol, 29.2 ml) and benzaldehyde (0.3 mol, 31.4 ml) in acetic anhydride (50 ml) was refluxed for 16 h. After cooling, the solution was poured into 200 ml of cold water and the mixture was made alkaline (pH = 8—9) with a 40% aqueous solution of sodium hydroxide. Brown precipitates were isolated by filtration and dried under vacuum. Repeated sublimation and a final recrystallization in hexane of the resulting solid gave white needles.

Anal. Calcd for $C_{13}H_{11}N$ (M = 181.24): C, 86.15; H, 6.12; N, 7.73%. Found: C, 86.21; H, 6.08; N, 7.68%.

***cis*-4-Styrylpyridine:**[18] To a solution of sodium ethoxide (0.17 mol, 11.57 g) in absolute ethanol (400 ml) was added, with vigorous stirring in nitrogen atmosphere, benzyltriphenylphosphonium chloride (0.194 mol, 84.2 g), followed by 4-pyridinealdehyde (0.154 mol, 16.5 g). The resulting mixture was stirred for 60 h, poured into 1000 ml of ice-water, and extracted with diethyl ether (4×100 ml). After the combined ether extract was washed with 200 ml of cold water, it was dried over anhydrous magnesium sulfate. The filtrate concentrated gave a pale-yellow residue, which was then slurried with 100 ml of petroleum ether. The slurry was filtered and the filtrate was concentrated. The resulting compound was a colorless liquid. Anal. Calcd for $C_{13}H_{11}N\cdot0.2H_2O$ (M = 184.84): C, 84.47; H, 6.22; N, 7.58%. Found: C, 84.80; H, 6.10; N, 7.48%.

[Fe(salten)(L)]BPh_4:[8a] Mononuclear iron(III) complexes with *trans*-4-styrylpyridine (*trans*-stpy) or *cis*-4-styrylpyridine (*cis*-stpy) were obtained by mixing [Fe(salten)Cl] with sodium tetraphenylborate. The synthesis of the *trans*-stpy complex **2** is exemplified in detail. To a solution of [Fe(salten)Cl] (1 mmol, 0.43 g) in methanol (50 ml) was added an excess of *cis*-stpy (1.5 mmol, 0.27 g). The mixture was warmed at 60 °C for 10 min and then filtered. The filtrate was added to a solution of sodium tetraphenylborate (1.3 mmol, 0.44 g) in methanol (10 ml). The mixture was warmed at 60 °C for 5 min and concentrated. The crude products were recrystallized from acetone/ethanol (1 : 1) with the addition of a small amount of *cis*-stpy ligand, and left standing overnight to precipitate violet crystals. They were collected, and then washed with methanol and diethyl ether.

Physical Measurements. Elemental analyses for carbon, hydrogen and nitrogen were performed at the Service Center of Elemental Analysis of Kyushu University. An iron analysis was made with an atomic absorption spectrophotometer, (AA-625-11 ; Shimadzu).

Magnetic Susceptibilities. The magnetic susceptibilities of the powder samples were measured by the Faraday method using a type 2002 (Cahn Instrument) electrovalence with an electromagnet (0.8 T).[19] $HgCo(NCS)_4$ was used as a calibration standard. Effective magnetic moments were calculated using the formula $\mu_{eff} = \sqrt{8\chi_M T}$, where χ_M is the molar magnetic susceptibility after applying a diamagnetic correction. The magnetic susceptibilities of the complexes in acetonitrile were measured by the Gouy method.

Mössbauer Spectra. Mössbauer spectra were measured with a constant-acceleration spectrometer (Austin Science Associates).[19] A cobalt-57 source of 10 mCi diffused into palladium foil was used for an absorption measurement. The spectra were fitted to a Lorentzian line shape using software of IGOR Pro (Wave Metrics, Inc.) on a personal computer. The isomer shifts and velocity scales were normalized to iron foil enriched with ^{57}Fe at room temperature.

Photochemical Measurements. The absorption spectra of the samples (5×10^{-5} mol dm^{-3}) in acetonitrile solution were recorded by using a UV-3100PC scanning spectrophotometer (Shimadzu) in the region from 200 to 800 nm. Irradiation at 313 nm was performed with a high-pressure mercury lamp using color filter glass UV-D33S (Toshiba), and irradiation at 460 nm with a halogen lamp AT-100HG (Shimadzu), using color filter glass L-42 (Toshiba). Irradiation for the solution was performed with stirring using a magnetic stirrer.

Single Crystal X-Ray Structural Analyses. The single-crystal structures of complexes **1** and **2** were determined.[19b] Complex **1** is described in detail because the *R* value of the structure analysis for **2** was large.

Data Collection. A violet prismatic crystal of **1** having approximate dimensions of about $0.20\times0.10\times0.30$ mm was mounted on a glass fiber. All measurements were made on a Rigaku AFC7R diffractometer with graphite monochromated Mo $K\alpha$ radiation and a 12 kW rotating anode generator. The data were collected at room temperature using the ω–2θ scan technique to a maximum 2θ value of 55.0°. Omega scans of several intense reflections, made prior to data collection, had an average width at a half-height of 0.34° with a take-off angle of 6.0°. Scans of (1.26+0.30 tan θ)° were made at a speed of 16.0° min^{-1} (in omega). The weak reflections ($I < 10.0\sigma(I)$) were rescanned (maximum of 4 scans) and the counts were accumulated to ensure good counting statistics. Stationary background counts were recorded on each side of the

reflection. The ratio of the peak counting time to the background counting time was 2 : 1. The diameter of the incident beam collimator was 1.0 mm, the crystal to detector distance was 235 mm, and the computer controlled detector aperture was set to 9.0×13.0 mm (horizontal×vertical).

Data Reduction. Of the 10690 reflections which were collected, 10287 were unique (R_{int} = 0.074). The intensities of three representative reflection were measured after every 150 reflections. No decay correction was applied. The linear absorption coefficient (μ) for Mo $K\alpha$ radiation is 3.3 cm^{-1}. An empirical absorption correction based on azimuthal scans of several reflections was applied, which resulted in transmission factors ranging from 0.24 to 1.00. The data were corrected for Lorentz and polarization effects.

Structure Solution and Refinement. The structures were solved by a direct method and expanded using Fourier techniques. The non-hydrogen atoms were refined anisotropically. Hydrogen atoms were included, but not refined. The final cycle of full-matrix least-squares refinement was based on 3889 observed reflections ($I > 3.00\sigma(I)$) and 657 variable parameters and converged (largest parameter was 1.27 times its esd) with unweighted and weighted agreement factors of:

$$R = \sum ||F_o| - |F_c|| / \sum |F_o| = 0.140,$$

$$R_w = \left[\sum w(|F_o| - |F_c|)^2 / \sum wF_o^2\right]^{\frac{1}{2}} = 0.172.$$

The standard deviation of an observation of unit weight was 3.20. The weighting scheme was based on counting statistics and included a factor (p = 0.007) to downweight the intense reflections. Plots of $\sum w(|F_o| - |F_c|)^2$ versus $|F_o|$, reflection order in data collection, $\sin\theta/\lambda$ and various classes of indices showed no unusual trends. The maximum and minimum peaks on the final difference Fourier map corresponded to 1.82 and −1.25 e^- $Å^{-3}$, respectively. Neutral atom-scattering factors were taken from Cromer and Waber. Anomalous dispersion effects were included in F_{calc}; the values for $\Delta f'$ and $\Delta f''$ were those of Creagh and McAuley. The values for the mass attenuation coefficients are those of Creagh and Hubbel. All calculations were performed using the teXsan crystallographic software package of Molecular Structure Corporation. (Crystallographic data have been deposited at the CCDC, 12 Union Road, Cambridge CB2 1EZ UK and copies can be obtained on request, free of charge, by quoting the publication citation and the deposition numbers CCDC 148066, 148067.) The complete $F_o - F_c$ data are deposited as Document No 73052 at the Office of the Editor of Bull. Chem. Soc. Jpn.

References

1 Y. Tanabe and S. Sugano, *J. Phys. Soc. Jpn.*, **9**, 753 (1954).

2 a) T. Kambara, *J. Chem. Phys.*, **70**, 4199 (1979). b) T. Kambara, *J. Chem. Phys.*, **74**, 4557 (1981).

3 Y. Maeda and Y. Takashima, *Comments Inorg. Chem.*, **7**, 41 (1988).

4 A. J. Conti, R. K. Chadha, K. M. Sena, A. L. Rheingold, and D. N. Hendrickson, *Inorg. Chem.*, **32**, 2670 (1993).

5 a) S. Decurtins, P. Gütlich, C. P. Köhler, H. Spiering, and A. Hauser, *Chem. Phys. Lett.*, **105**, 1 (1984). b) S. Decurtins, P. Gütlich, K. M. Hasselbach , A. Hauser, and H. Spiering, *Inorg. Chem.*, **24**, 2174 (1985). c) P. Gütlich, A. Hauser, and H. Spiering, *Angew. Chem., Int. Ed. Engl.*, **33**, 2024 (1994). d) P. Gütlich and A. Hauser, *Coord. Chem. Rev.*, **97**, 1 (1990).

6 a) O. Kahn, J. Kröber, and C. Jay, *Adv. Mater.*, **4**, 718 (1992). b) J. F. Letard, P. Guinonneau, L. Rabardel, J. A. K. Howard, A. E. Goeta, D. Chasseau, and O. Kahn, *Inorg. Chem.*, **37**, 4432 (1998). c) J. A. Real, E. Andres, M. C. Munoz, M. Julve, T. Granier, A. Bousseksou, and F. Varret, *Science*, **268**, 265 (1995). d) J. A. Real, M. C. Munoz, J. Faus, and X. Solans, *Inorg. Chem.*, **36**, 3008 (1997).

7 a) J. Zarembowitch, C. Roux, M.-L. Boillot, R. Claude, J.-P. Itié, A. Polian, and M. Bolte, *Mol. Cryst. Liq. Cryst.*, **234**, 247 (1993). b) C. Roux, J. Zarembowitch, B. Gallois, T. Granier, and R. Claude, *Inorg. Chem.*, **33**, 2273 (1994). c) M.-L. Boillot, C. Roux, J.-P. Audiére, A. Dausse, and J. Zarembowitch, *Inorg. Chem.*, **35**, 3975 (1996).

8 a) N. Matsumoto, S. Ohta, C. Yoshimura, A. Ohyoshi, S. Kohata, H. Okawa, and Y. Maeda, *J. Chem. Soc., Dalton Trans.*, **1985**, 2575. b) S. Ohta, C. Yoshimura, N. Matsumoto, H. Okawa, and A. Ohyoshi, *Bull. Chem. Soc. Jpn.*, **59**, 155 (1986). c) Y. Maeda, Y. Noda, H. Oshio, and Y. Takashima, *Bull. Chem. Soc. Jpn.*, **65**, 1825 (1992).

9 a) E. Sinn, G. Sim, E. V. Dose, M. F. Tweedle, and L. J. Wilson, *J. Am. Chem. Soc.*, **100**, 3375 (1978). b) T. Ito, M. Sugimoto, H. Ito, K. Toriumi, H. Nakayama, W. Mori, and M. Sekizaki, *Chem. Lett.*, **1983**, 121.

10 M. Blume, *Phys. Rev. Lett.*, **18**, 305 (1967).

11 S. Ohta, C. Yoshimura, N. Matsumoto, H. Okawa, and A. Ohyoshi, *Bull. Chem. Soc. Jpn.*, **59**, 155 (1986).

12 P. Bortolus, G. Cauzzo, U. Mazzucato, and G. Galiazzo, *Z. Phys. Chem. Neue Forge*, **51**, 264 (1966).

13 P. Bortolus, G. Cauzzo, U. Mazzucato, and G. Galiazzo, *Z. Phys. Chem. Neue Forge*, **63**, 29 (1969).

14 a) G. Bartocci, P. Bortolus, and U. Mazzucato, *J. Phys. Chem.*, **77**, 605 (1973). b) G. Bartocci, U. Mazzucato, F. Masetti, and G. Galiazzo, *J. Phys. Chem.*, **84**, 847 (1980). c) G. Bartocci and U. Mazzucato, *J. Lumin.*, **27**, 163.

15 U. Mazzucato, *Pure Appl. Chem.*, **54**, 1705 (1982).

16 F. Barigelletti, S. Dellonte, G. Orlandi, G. Bartocci, F. Masetti, and U. Mazzucato, *J. Chem. Soc., Faraday Trans. 1*, **80**, 1123 (1984).

17 C. Roux, J. Zarembowitch, B. Gallois, and M. Bolte, *New J. Chem.*, **16**, 671 (1992).

18 J. L. R. Williams, R. E. Adel, J. M. Carlson, G. A. Reynolds, D. G. Borden, and J. A. Ford, Jr., *J. Org. Chem.*, **28**, 387 (1963).

19 a) Y. Maeda, T. Manago, S. Hayami, H. Oshio, S. Osaki, H. Hasuyama, and R. H. Herber, *J. Chem. Soc., Dalton Trans.*, **1999**, 1001. b) The references for X-ray determination are included in this paper.